IMEKO, IEEE, SICE
2nd International Symposium on Measurement, Analysis and Modeling of Human Functions
1st Mediterranean Conference on Measurement
June 14-16, 2004, Genova, Italy

DEVELOPMENT OF A DIAGNOSIS SUPPORT SYSTEM ON VASCULAR CONDITIONS USING A PROBABILISTIC NEURAL NETWORK

Akira Sakane, Toshio Tsuji, and Yoshiyuki Tanaka
Department of Artificial Complex Systems Engineering
Hiroshima University
Kagamiyama 1-4-1, Higashi-Hiroshima, Hiroshima,
739-8527 JAPAN
Noboru Saeki and Masashi Kawamoto
Department of Anesthesiology and Critical Care
Hiroshima University
Kasumi 1-2-3, Minami-ku, Hiroshima,
734-8551 JAPAN

1. INTRODUCTION

A medical doctor needs to judge patient's conditions from biological signals such as electrocardiogram and blood pressure during operations quickly and properly. Since these biological signals include blood circulation information, the observation of patient's conditions through temporal changes of waveform is possible [1]. However, special knowledge for blood circulation and considerable experiences are necessary to notice subtle changes in the waveform, so it is very difficult for inexperienced doctors to judge the vascular conditions properly. Also, the doctors may be put a considerable mental strain when it is necessary for the patient's vital signs to be controlled for a long period of time, such as surgical operations. If a diagnosis support system on vascular conditions becomes available, the medical staff will be able to identify patient's conditions more easily.

The development of a diagnosis support system based on vascular conditions has not been reported so far, although a few similar studies on the estimation system of vascular aging have been reported [2],[3]. For example, Takada *et al.* examined the correlation between waveform of accelerated plethysmogram and aging by statistical procedure, and estimated the vascular aging [2]. However, the estimated age was not based on quantitative vascular characteristics. It is impossible to monitor the patient's conditions during operations using previously proposed methods.

On the other hand, vascular contraction or relaxation is controlled by smooth muscle cells in an arterial wall. Some studies used mechanical impedance to describe dynamic characteristics of biological systems quantitatively. Mechanical impedance consisting of stiffness, viscosity, and inertia, has been used to model mechanical characteristics of muscles in previous studies. Mussa Ivaldi *et al.* pioneered the measurement of human hand stiffness, and examined the hand stiffness in a stable arm posture [4]. Tsuji *et al.* estimated not only hand stiffness but also viscosity and inertia, and investigated human impedance under various conditions on muscle contraction levels, arm postures and motion directions [5], [6].

Some studies which modeled dynamic characteristics of arterial wall by using mechanical impedance have been also reported [7],[8]. Mascaro and Asada *et al.* estimated the impedance properties of the arterial wall from the velocity of blood flow and the arterial caliber, but did not discuss its validity and accuracy [7]. Saeki *et al.* estimated compliance of the arterial wall only by using a plethysmogram and blood pressure measurements [8]. We had proposed a method to express the dynamic characteristics of the arterial wall using mechanical impedance by applying a muscle impedance estimation method [5], and estimated the arterial wall impedance during operations [9]. Also, we have succeeded to discriminate the vascular conditions by using the estimated impedance parameters [10]. However, the discrimination result only showed one of two conditions as "Normal" and "Vasoconstriction," and the result was not enough to judge the vascular conditions in spite of the off-line discrimination of the vascular conditions. Accordingly, this off-line estimation method can not be applied to the actual surgical operation.

As the first step to diagnose the vascular conditions on-line, this paper aims to discriminate vascular conditions from changes of biological signals and arterial wall impedance using a probabilistic neural network, and apply it to monitor the vascular conditions toward developing an on-line diagnosis support system. In this paper, section 2 explains the discrimination method of vascular conditions and introduces the summary of the proposed system. In section 3, the experimental results are shown, and conclusions are given in section 4.

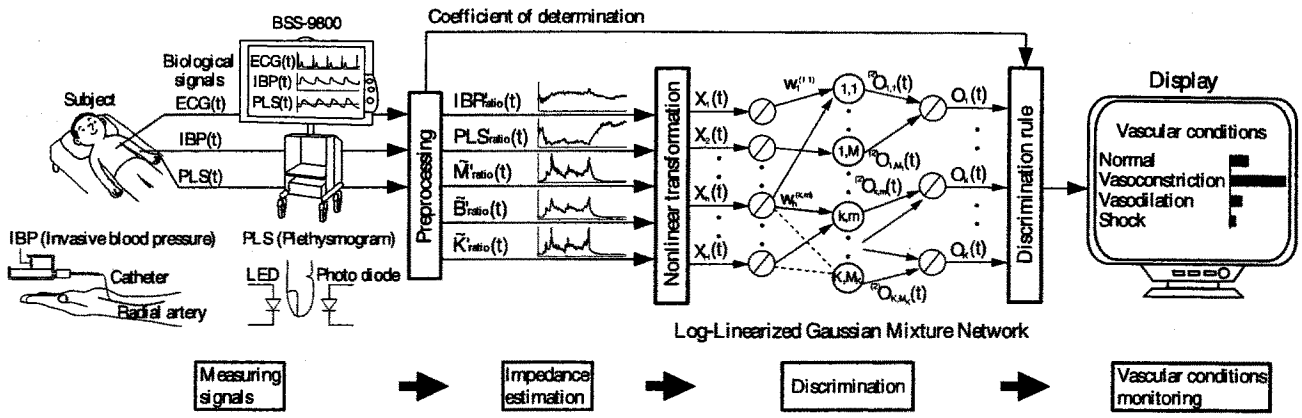

Fig. 1. A diagnosis support system on vascular conditions

2. VASCULAR CONDITIONS DIAGNOSIS SUPPORT SYSTEM

A structure of the proposed diagnosis support system is shown in Fig.1. In the proposed system, we used Log-Linearized Gaussian Mixture Network (LLGMN) [11], based on a log-linear model and a Gaussian mixture model for discrimination. The methods of preprocessing and discriminating vascular conditions are described below.

2.1. Preprocessing

For extracting features including biological signals, we estimated the arterial wall impedance [9]. Fig. 2 illustrates the proposed impedance model of the arterial wall. This model represents only the characteristics of the arterial wall in the arbitrary radius direction. The impedance characteristic can be described using an external force and a displacement of the radius of arterial wall as follows:

$$F(t) = M\ddot{r}(t) + B\dot{r}(t) + K(r(t) - r_e) \tag{1}$$

where $F(t)$ is the force exerted on the arterial wall by blood flow; M, B, and K are the inertia, viscosity, and stiffness; $r(t), \dot{r}(t)$, and $\ddot{r}(t)$ are the position, velocity, and acceleration of the wall; and r_e denotes the equilibrium vascular radius when blood pressure is zero. The vascular dynamic characteristic at the time t can be derived as follows:

$$dF(t) = Md\ddot{r}(t) + Bd\dot{r}(t) + Kdr(t) \tag{2}$$

where $dr(t) = r(t) - r(t_0); d\dot{r}(t) = \dot{r}(t) - \dot{r}(t_0); d\ddot{r}(t) = \ddot{r}(t) - \ddot{r}(t_0); dF(t) = F(t) - F(t_0)$; and t_0 denotes the start time just at moving arterial walls.

To estimate the impedance parameters given in (2), it is necessary to measure $F(t)$ and $r(t)$. Assuming that the force $F(t)$ is proportional to blood pressure $P_b(t)$, the following equation can be obtained:

$$F(t) = k_f P_b(t) \tag{3}$$

where k_f is a proportional constant [9].

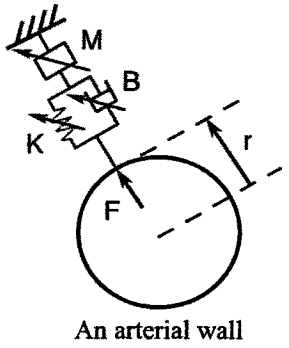

Fig. 2. An arterial wall impedance model

On the other hand, the vascular radius $r(t)$ is quite difficult to measure directly. So, in this paper, a plethysmogram is utilized instead of $r(t)$.

Let I_0 denote the intensity of incident light on a blood vessel with diameter D, and I_D means the intensity of light transmitted through the apex of the finger. According to Lambert-Beer's law [12], the following equation can be obtained:

$$A_D \equiv \log(I_0/I_D) = ECD \tag{4}$$

where A_D is the optical density that is proportional to the concentration of absorptive substance C and the diameter of a blood vessel D. E is the peculiar absorptive constant for each material. If the case that the caliber of a blood vessel D changes $D + \Delta D(t)$ and the light transmitted through the apex of the finger becomes $I_D - \Delta I(t)$, the variation of optical density $\Delta A(t)$ can be given by

$$\begin{aligned} \Delta A(t) &= A(t) - A_D \\ &= \log(I_D/(I_D - \Delta I(t))) = EC\Delta D(t). \end{aligned} \tag{5}$$

The variation of optical density $\Delta A(t)$ is defined as the plethysmogram $P_l(t)$.

The value of plethysmogram changes proportional to the pulsation of blood vessels. In this paper, it is assumed that vascular radius $r_v(t)$ is proportional to the plethysmogram:

$$r_v(t) = \frac{P_l(t) + A_D}{k_p} \tag{6}$$

where k_p is a proportional constant.

The force exerted on the arterial wall is expressed by the arterial pressure $P_b(t)$ given by (3), and the vascular radius $r_v(t)$ is represented by the plethysmogram $P_l(t)$ in (6). Then, the arterial wall impedance is estimated by using $P_b(t)$ and $P_l(t)$ as follows:

$$dP_b(t) = \tilde{M}d\ddot{P}_l(t) + \tilde{B}d\dot{P}_l(t) + \tilde{K}dP_l(t) \tag{7}$$

where $dP_b(t) = P_b(t) - P_b(t_0)$; and $dP_l(t) = P_l(t) - P_l(t_0)$. The impedance parameters included in (7) are then given by

$$\tilde{M} = \frac{M}{k_p k_f}, \tilde{B} = \frac{B}{k_p k_f}, \tilde{K} = \frac{K}{k_p k_f} \tag{8}$$

where the parameter $\tilde{M}$ corresponds to the mass of the arterial wall existing in the measured part; $\tilde{B}$ and $\tilde{K}$ to the viscoelastic properties, respectively [9].

Fig.3 shows an example of the measured electrocardiogram ($ECG(t)$), blood pressure ($IBP(t)$), and plethysmogram ($PLS(t)$). ECG includes P waves (atrial depolarization), Q waves, R waves, S waves (ventricular depolarization and contraction), and T waves (ventricular repolarization) in general [13]. In the proposed method, the estimation period of the arterial wall impedance is the time between successive R-peaks (an RR interval), where the peak of the R wave can be detected from ECG signals. After determining the estimation period, the impedance parameters $\tilde{M}$, $\tilde{B}$, and $\tilde{K}$ are estimated by substituting $dP_b(t)$ and $dP_l(t)$ into (7), where $dP_b(t)$ and $dP_l(t)$ are the variations of blood pressure and plethysmogram from the detecting time of R wave t_0. Because the time needed for estimating arterial wall impedance is smaller than the RR interval, it is possible to estimate the arterial wall impedance "beat-to-beat."

When vascular conditions are discriminated, proportional coefficients k_f and k_p included in the impedance model cause difficulty in discriminating the vascular conditions. To reduce the effect of these coefficients, an impedance ratio can be used. The impedance ratios $\tilde{M}_{\text{ratio}}$, $\tilde{B}_{\text{ratio}}$, and $\tilde{K}_{\text{ratio}}$ are calculated for $\tilde{M}$, $\tilde{B}$, and $\tilde{K}$ as follows:

$$\tilde{M}_{\text{ratio}} = \frac{\tilde{M}}{\tilde{M}_{\text{rest}}}, \tilde{B}_{\text{ratio}} = \frac{\tilde{B}}{\tilde{B}_{\text{rest}}}, \tilde{K}_{\text{ratio}} = \frac{\tilde{K}}{\tilde{K}_{\text{rest}}} \tag{9}$$

where $\tilde{M}_{\text{rest}}$, $\tilde{B}_{\text{rest}}$, and $\tilde{K}_{\text{rest}}$ are the nominal values of impedance ratios when patients are in a relatively rested condition.

Similarly, the ratios of blood pressure and plethysmogram are calculated as follows:

$$IBP_{\text{ratio}} = \frac{IBP_{\max} - IBP_{\min}}{IBP_{\text{rest}}}, PLS_{\text{ratio}} = \frac{PLS_{\max} - PLS_{\min}}{PLS_{\text{rest}}} \tag{10}$$

where $IBP_{\max}$, $IBP_{\min}$, $PLS_{\max}$, and $PLS_{\min}$ are maximum and minimum values of blood pressure and plethysmogram divided into beat-to-beat; IBP_{rest} and PLS_{rest} are maximum and minimum value differences of blood pressure and plethysmogram in a relatively rested condition.

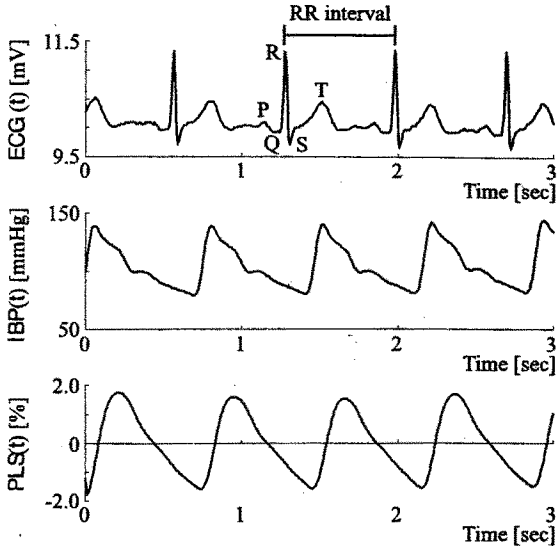

Fig. 3. Example of the measured electrocardiogram, blood pressure, and plethysmogram. The electrocardiogram consists of P waves, Q waves, R waves, S waves, and T waves in general.

A neural network is used to discriminate the vascular conditions using the normalized ratios of impedance and biological signals given by

$$\begin{aligned} \tilde{M}'_{\text{ratio}} &= \frac{\tilde{M}_{\text{ratio}}}{k_{\text{M}}}, \tilde{B}'_{\text{ratio}} = \frac{\tilde{B}_{\text{ratio}}}{k_{\text{B}}}, \tilde{K}'_{\text{ratio}} = \frac{\tilde{K}_{\text{ratio}}}{k_{\text{K}}}, \\ IBP'_{\text{ratio}} &= \frac{IBP_{\text{ratio}}}{k_{\text{I}}}, PLS'_{\text{ratio}} = \frac{PLS_{\text{ratio}}}{k_{\text{P}}} \end{aligned} \tag{11}$$

where the gains for normalization, k_{M}, k_{B}, k_{K}, k_{I}, and k_{P}, are determined by the maximum value of each estimated signal in advance.

The LLGMN receives the impedance and biological signals ratios from (11) as characteristics vector $\boldsymbol{x}(t) = [x_1(t),\ x_2(t),\ \cdots,\ x_L(t)]^{\text{T}} \in \Re^L (L = 5)$.

2.2. Neural Network Structure

The structure of the LLGMN [11] is shown in Table I. This network is of a feedforward type and contains three layers. First, the input feature vector $\boldsymbol{x}(t)$ is transformed into the modified input vector $\boldsymbol{X}(t) \in \Re^H (H = 1 + L(L+3)/2)$ in order to represent the probability density function corresponding to each component of the Gaussian Mixture Model (GMM) [14] as a nonlinear combination of $\boldsymbol{X}(t)$:

$$\begin{aligned} \boldsymbol{X}(t) = [&1,\ \boldsymbol{x}(t)^{\text{T}},\ x_1(t)^2,\ x_1(t)x_2(t),\ \cdots, \\ &x_1(t)x_L(t),\ x_2(t)^2,\ x_2(t)x_3(t), \\ &\cdots,\ x_2(t)x_L(t),\ \cdots,\ x_L(t)^2]^{\text{T}} \end{aligned} \tag{12}$$

The first layer consists of H units corresponding to the dimension of $\boldsymbol{X}(t)$, and the identity function is used for activation of each unit.

The second layer consists of the same number of units as the total component number of the GMM. Each unit receives

TABLE I
STRUCTURE OF THE LLGMN.

The 1st layer	Number of units	H
	Input	$X_h(t)$
	Output	$^{(1)}O_h(t)$
	I/O function	Identity function
The 2nd layer	Number of units	$\sum_{k=1}^{K} M_k$
	Input	$^{(2)}I_{k,m}(t) \sum_{h=1}^{H} {}^{(1)}O_h(t) w_h^{(k,m)}$
	Output	$^{(2)}O_{k,m}(t)$
	I/O function	Generalized sigmoid function
The 3rd layer	Number of units	K
	Input	$^{(3)}I_k(t) \sum_{m=1}^{M_k} {}^{(2)}O_{k,m}(t)$
	Output	$^{(3)}O_k(t)$
	I/O function	Identity function
Weight coefficients from 1st layer to 2nd layer		$w_h^{(k,m)}$
Weight coefficients from 2nd layer to 3nd layer		1

the output of the first layer weighted by the coefficient $w_h^{(k,m)}$ and outputs the posteriori probability of each component. The input to the unit $\{k,m\}$ in the second layer, $^{(2)}I_{k,m}(t)$, and the output $^{(2)}O_{k,m}(t)$ are defined as

$$^{(2)}I_{k,m}(t) = \sum_{h=1}^{H} {}^{(1)}O_h(t) w_h^{(k,m)} \tag{13}$$

$$^{(2)}O_{k,m}(t) = \frac{\exp[^{(2)}I_{k,m}(t)]}{\sum_{k'=1}^{K} \sum_{m'=1}^{M_{k'}} \exp[^{(2)}I_{k',m'}(t)]} \tag{14}$$

where $^{(1)}O_h(t)$ denotes the output of the h-th unit in the first layer, and $w_h^{(K,M_K)} = 0$ $(h = 1, 2, \cdots, H)$. It should be noted that (14) can be considered as a kind of the generalized sigmoid functions.

Finally, the third layer consists of K units corresponding to the number of classes, and outputs the posteriori probability of the class k $(k = 1, 2, \cdots, K)$. The unit k integrates the outputs of M_k units $\{k,m\}$ $(m = 1, 2, \cdots, M_k)$ in the second layer. The relationship between the input and the output is defined as

$$^{(3)}I_k(t) = \sum_{m=1}^{M_k} {}^{(2)}O_{k,m}(t) \tag{15}$$

$$^{(3)}O_k(t) = {}^{(3)}I_k(t) \tag{16}$$

In the LLGMN defined above, the *a posteriori* probability of each class is defined as outputs of the last layer. Note that the log-linearized Gaussian mixture structure is incorporated into the network by learning the weight coefficients $w_h^{(k,m)}$ [11].

Next, let us consider the supervised learning with the teacher vector $\boldsymbol{T}(n) = [T_1(n), T_2(n), \cdots, T_K(n)]^{\mathrm{T}}$ for the nth input vector $\boldsymbol{x}(n)$. When the teacher provides perfect classification,

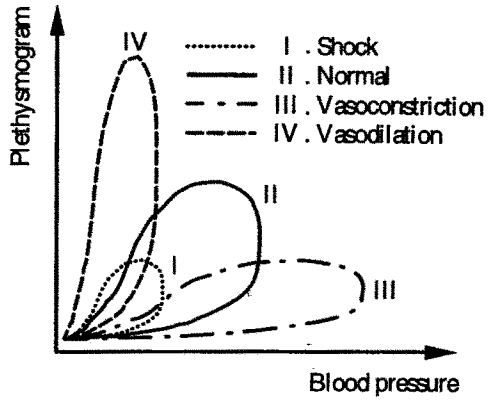

Fig. 4. Biological signals and vascular conditions.

TABLE II
VASODILATION AND SHOCK CONDITIONS.

Vascular conditions	IBI'_{ratio}	PLS'_{ratio}	$\tilde{M}'_{ratio}$	$\tilde{B}'_{ratio}$	$\tilde{K}'_{ratio}$
Vasodilation	0.12	0.75	0.006	0.006	0.006
Shock	0.08	0.10	0.033	0.033	0.033

$T_k(n) = 1$ for the particular class k and $T_k(n) = 0$ for all the other classes. As an energy function for the network, we use

$$J = -\sum_{n=1}^{N} \sum_{k=1}^{K} T_k(n) \log O_k(n) \tag{17}$$

and the learning is performed to minimize J [11], that is, to maximize the likelihood.

2.3. Discrimination Rule

When vascular conditions are discriminated by the NN, any misclassification may have a critical effect on patients. To prevent such a misclassification, a coefficient of determination is used to judge whether the discrimination is able to be performed. The coefficient of determination indicates how the model can adequately describe vascular characteristics [9].

First, the coefficient of determination is calculated from the measured arterial pressure and estimated arterial pressure using (7). Next, the coefficient of determination R^2 and the threshold R_d^2 are compared to suspend the discrimination based on the coefficient of determination. For example, if $R^2 \geq R_d^2$, the discriminated result is selected as vascular condition. On the other hand, the discrimination should be suspended if $R^2 < R_d^2$. Thus, possible misclassifications are expected to be reduced.

2.4. Vascular Conditions

In this paper, we defined the four vascular conditions ($K = 4$): i.e., 1) normal, 2) vasoconstriction, 3) vasodilation, and 4) shock which are shown in a Lissajous figure (Fig.4) [8]. The vertical axis represents the blood pressure, and the horizontal axis indicates the plethysmogram. The doctors can judge the patient's vascular conditions from each waveform [8]. The vascular conditions for discrimination are defined as follows:

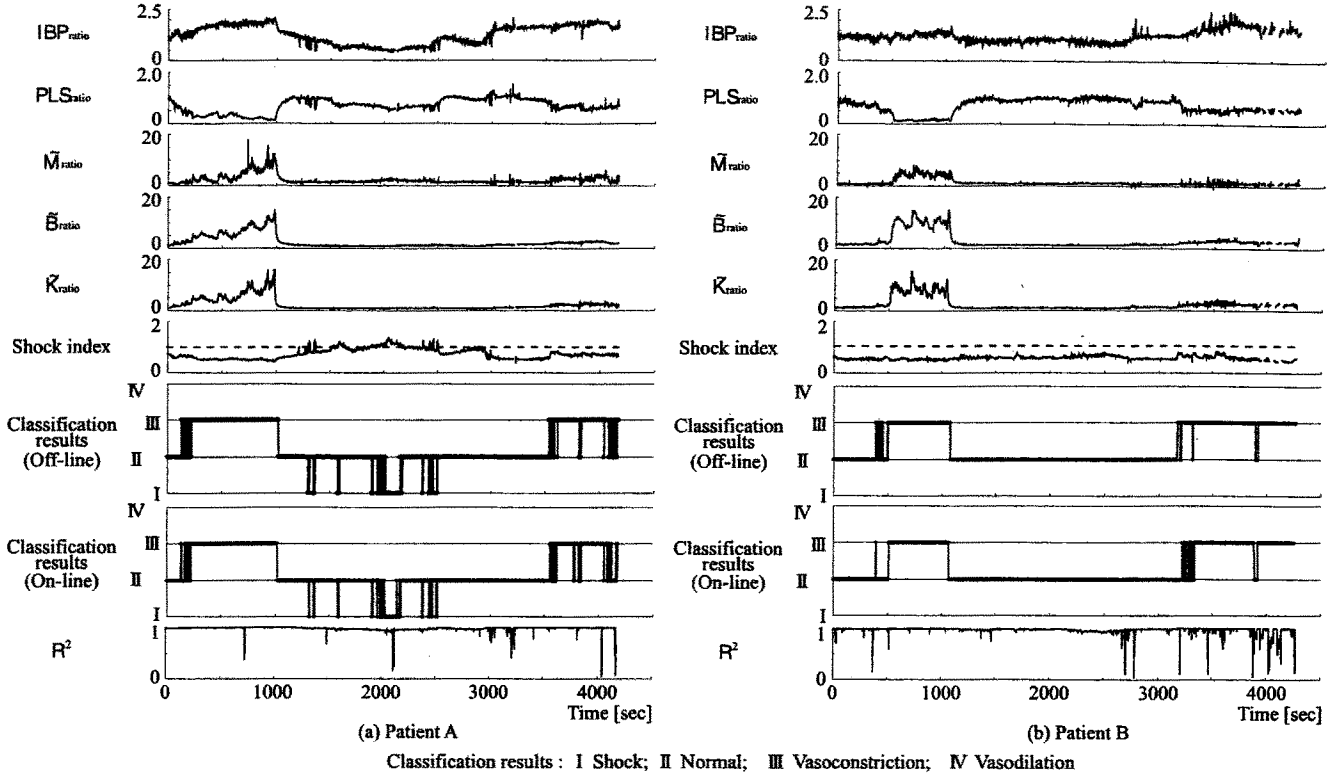

Fig. 5. Classification results of the vascular conditions during surgical operations in off-line and on-line processing.

I. **Shock** A condition due to inadequate blood supply to tissues which is life-threatening.

II. **Normal** Good blood circulation.

III. **Vasoconstriction** It decreases the diameter of the vessel lumen to allow less blood through. This is caused by the dilation or contraction of the smooth muscle in the vessel walls, particularly in the arterioles.

IV. **Vasodilation** It is the process by which blood vessels are dilated in the extremities (arms and legs), allowing a greater volume of blood to flow to these tissues (It is the exact opposite to the Vasoconstriction).

3. DISCRIMINATION EXPERIMENT

3.1. Experimental Condition

The proposed method is applied to discriminate the vascular conditions. The subjects were operated on using the endoscopic transthoracic sympathectomy for hyperhidrosis (Patient A and B). If a blood vessel contracts due to stimulation from sympathetic nerves, the palms and armpits will perspire. In this operation, the sympathetic nerves on the sides of the backbone are interrupted using a clip to stop the perspiration [16]. After that, strong stimulations are not given normally. When the sympathetic nerve is interrupted, a blood vessel becomes compliant on the spot. Therefore, if the vascular conditions can be identified on-line, it is possible to ascertain its success or failure during operation.

Electrocardiogram ($ECG(t)$), arterial pressure ($P_b(t)$), and plethysmogram ($P_l(t)$) were measured at 125 [Hz] simultaneously for discriminating vascular conditions. The arterial pressure was measured through a catheter (24 gauge) placed in the left radial artery, and the plethysmogram was measured with the ipsilateral forefinger (BSS-9800, NIHON KOHDEN Co., Ltd).

In this study, we wanted to discriminate the vascular conditions on-line, and validate their availability during operations. However, at the present time, it is almost impossible to apply the proposed method during actual operations because of ethical problems. Therefore, we constructed the on-line discrimination environment in LabVIEW (National Instruments Co., Ltd), and verified the classification possibility on-line by estimating vascular conditions from the measured data in advance "beat-to-beat."

The learning data was created from that of the four patients (non-subjects) who operated the endoscopic transthoracic sympathectomy for hyperhidrosis patients. However, the learning data of the "Vasodilation" and "Shock" conditions were not available from the patients. Such unobservable facts were represented randomly by normal distribution with $N(\mu, 0.005)$. The means μ of "Vasodilation" and "Shock" conditions are shown in Table II.

3.2. Experimental Results

Fig.5 shows the result of discrimination experiments. Time profiles of the ratio of blood pressure, the ratio of plethysmogram, the ratio of inertia, the ratio of viscosity, the ratio of stiffness, the shock index (SI), the classification results (off-line and on-line), and coefficient of determination are shown in order from the top. The shock index was used for comparing to

the "Shock" condition discriminated by the proposed method based on the vascular conditions. This index is calculated from the ratio of heart rate to systolic arterial pressure; "Normal" condition at 0.6; while "Shock" condition over 1.0 [17].

The blood vessels become stiff in the shaded areas. The nominal values of impedance and biological signals are an average of consecutive 10 sample data after the patients are under anesthesia. The discrimination threshold of vascular conditions is settled at $R_d^2 = 0.9$, and the discrimination is suspended when the coefficient of determination R^2 is less than 0.9. Also, the normalization gains included in (11) are set as follows: $k_M = k_B = k_K = 30.0, k_I = 2.5, k_P = 2.0$.

In Fig.5(a), the estimated impedance shows that the blood vessels gradually became stiff because the doctor stimulated the patient's tissues to find the sympathetic nerves at 200 ~1000 [sec], and NN discriminated the vascular condition as "Vasoconstriction". After 1000 [sec], the blood vessels became compliant, and vascular condition was discriminated as "Normal". After that, the ratios of blood pressure and plethysmogram gradually decreased, the vascular condition was discriminated as "Shock", and the corresponding shock index was indicated as equal or greater than 1.0 at the same time. Also, when the effect of the anesthesia wore off after 3500[sec] and blood vessels became stiff, the vascular condition was discriminated as "Vasoconstriction". By using the ratios of arterial wall impedance and biological signals, the vascular conditions with operative techniques can be discriminated well.

In the result of Fig.5(b), the patient B was stimulated around 500~1000 [sec], and the effect of anesthesia wore off after 3300 [sec], where the NN discriminated the vascular condition as "Vasoconstriction" adequately. In this figure, the discrimination results were influenced by external factors when the anesthesia wore off. In the future research, it should be considered how to determine the threshold level of the coefficient of determination. Although in each patient, similar discrimination results were observed both on and off-line, and the usefulness of the proposed method was validated because the vascular conditions could be discriminated.

4. CONCLUSION

This paper proposed a new method to discriminate the vascular conditions by using a probabilistic neural network, and developed the diagnosis support system to judge the patient's conditions. The discrimination was applied to the measured data in the surgical operations, and the vascular conditions could be discriminated with high accuracy using the proposed method. Furthermore, it was revealed that the discrimination results on-line were similar to the discrimination results off-line.

Future research will be directed to measure the biological signals and discriminate the vascular conditions on-line. Also, for the application to surgical operations, the development of easy-to-use interface for doctors is necessary.

ACKNOWLEDGMENT

The authors would like to thank T.Ukawa and K.Tone of the NIHON KOHDEN Co., Ltd for making available clinical data and for their precious suggestions.

This work was supported by Grant-in-Aid for Scientific Research of Japan Society for the Promotion of Science (15008279).

REFERENCES

[1] D.E.Longnecker and F.L.Murphy, Introduction to Anesthesia, Elsevier Science Health Science div, 1997.

[2] H.Takada, S.M.Mirbod, and H.Iwata, "The relative vascular age derived from acceleration plethysmogram: A new attempt.," *Jpn. J. Appl. Physiol.*, Vol. 28, No. 2, pp. 115-121, 1998.

[3] Y.Maniwa, T.Iokibe, M.Koyama, M.Yamamoto, and S.Ohta, "The Application of Pulse Wave Chaos in Clinical Medicine," *in Proc. 17th FUZY System Symposium*, Chiba, pp. 787-790, 2001.

[4] F.A.Mussa-Ivaldi, N.Hogan, and E.Bizzi, "Neural, mechanical and geometrical factors sub-serving arm posture in humans," *Journal of Neuroscience*, Vol. 5, No. 10, pp. 2732-2743, 1985.

[5] T.Tsuji, P.G.Morasso, K.Goto, and K.Ito, "Human hand impedance characteristics during maintained posture," *Biol. cybern.*, Vol. 72, pp. 457-485, 1995.

[6] T.Tsuji and M.Kaneko, "Estimation and Modeling of Human Hand Impedance during Isometric Muscle Contraction," *in Proc. ASME.*, DSC-Vol. 58, pp. 575-582, Atlanta, 1996.

[7] A.Mascaro, and H.Asada, "Photoplethysmograph Fingernail Sensors for Measuring Finger Forces Without Haptic Obstruction," *IEEE Trans. Robot. Automat.*, Vol. 17, No. 5, pp. 698-708, 2001.

[8] N.Saeki, M.Kawamoto, and O.Yuge, "Quantitative view of peripheral circulation," *Critical Care Medicine*, Vol. 28, No. 12, A62(suppl), 2000.

[9] A.Sakane, T.Tsuji, Y.Tanaka, N.Saeki, and M.Kawamoto, "Estimating Arterial Wall Impedance using a Plethysmogram," *in Proc. 29th Annual Conference of the IEEE Industrial Electronics Society*, Roanoke, Virginia, USA, pp. 580-585, 2003.

[10] A.Sakane, T.Tsuji, N.Saeki, and M.Kawamoto, "Discrimination of Vascular Conditions using a Probabilistic Neural Network," *Journal of Robotics and Mechatronics*, Vol. 16, No. 2, 2004 (in press).

[11] T.Tsuji, O.Fukuda, H.Ichinobe, and M.Kaneko, "A Log-Linearized Gassian Mixture Network and Its Application to EEG Pattern Classification," *IEEE Trans. Syst., Man, Cybern-Part C, Appl. and Rev.*, Vol. 29, No. 1, pp. 60-72, 1999.

[12] R.A.Day and A.L.Underwood, QUANTITATIVE ANALYSIS 4th Edition, Prentice-Hall, 1980.

[13] M.J.Goldman, Principles of Clinical Electrocardiography, Prentice Hall, 1986.

[14] J.H.Wolfe, "Pattern clustering by multivariate mixture analysis," *Multivariate Behavioral Res.*, vol. 5, pp. 329-350, 1970.

[15] J.Archdeacon, Correlation and Regression Analysis, Univ of Wisconsin Pr, 1994.

[16] C.Drott, G.Gothberg, and G.Claes, "Endoscopic transthoracic sympathectomy: An efficient and safe method for the treatment of hyperhidrosis," *Journal of the American Academy of Dermatology*, Vol. 33, pp. 78-81, 1995.

[17] MY.Rady, P.Nightingale, RA.Little, and JD.Edwards, "Shock index: a re-evaluation in acute circulatory failure," *Resuscitation*, Vol. 23, No. 3, pp. 227-234, 1992.

Author:

DEVELOPMENT OF A DIAGNOSIS SUPPORT SYSTEM ON VASCULAR CONDITIONS USING A PROBABILISTIC NEURAL NETWORK,

A.Sakane, T.Tsuji, and Y.Tanaka are with the Department of Artificial Complex Systems Engineering, Hiroshima University, 1-4-1 Kagamiyama, Higashi-Hiroshima, Hiroshima, 739-8527 Japan.

Phone: +81-824-24-7676, Fax: +81-824-22-7030,

E-mail: sakane@bsys.hiroshima-u.ac.jp, tsuji@bsys.hiroshima-u.ac.jp, ytanaka@bsys.hiroshima-u.ac.jp

N.Saeki and M.Kawamoto are with the Department of Anesthesiology and Critical Care, Hiroshima University, 1-2-3 Kasumi, Minami-ku, Hiroshima, 734-8551 Japan.

E-mail: nsaeki@hiroshima-u.ac.jp, anekawa@hiroshima-u.ac.jp